

Robust preconditioners for the high-contrast Stokes equation

BURAK AKSOYLU¹,

Department of Mathematics, TOBB University of Economics and Technology, Ankara, 06560, Turkey

Department of Mathematics, Louisiana State University, Baton Rouge, LA 70803, USA

ZUHAL UNLU

Department of Mathematics, Louisiana State University, Baton Rouge, LA 70803, USA

Abstract

We consider the Stokes equation with high-contrast viscosity coefficients. We construct a preconditioner that is robust with respect to contrast size and mesh size simultaneously based on the preconditioner proposed by Aksoylu et al. (2008). We examine the performance of our preconditioner against multigrid and provide a comparative study reflecting the effect of the underlying discretization and the aspect ratio of the mesh. We address the rigorous justification of the solver methods, p-Uzawa and p-Minres, used in Aksoylu and Unlu (2013), and compare the results with additional solver method, Schur complement reduction (SCR). We observe that our preconditioner is only contrast size robust under the p-SCR solver. The inexact p-Uzawa solver remains to be the best choice for the most effective performance of our preconditioner as we observe contrast size and mesh size robustness simultaneously in this case. As the contrast size grows asymptotically, we prove and numerically demonstrate that the inexact p-Uzawa solver converges to the exact one. Finally, we show that our preconditioner is contrast size and mesh size robust under p-Minres when the Schur complement solve is accurate enough.

Keywords: Stokes equation, high-contrast, high-contrast viscosity, robust preconditioning, Schur complement, singular perturbation analysis.

1. Introduction

In this paper, we consider the following stationary Stokes equation in a domain $\Omega \subset \mathbb{R}^2$:

$$\begin{aligned} -\nabla \cdot (\nu \nabla u) + \nabla p &= f && \text{in } \Omega, \\ \nabla \cdot u &= 0 && \text{in } \Omega, \end{aligned} \tag{1}$$

Email addresses: baksoylu@etu.edu.tr (BURAK AKSOYLU), zyeter1@math.lsu.edu (ZUHAL UNLU)

¹B. Aksoylu was supported in part by National Science Foundation DMS 1016190 grant, European Union Marie Curie Career Integration 293978 grant, and Scientific and Technological Research Council of Turkey (TÜBİTAK) TBAG 112T240 grant.

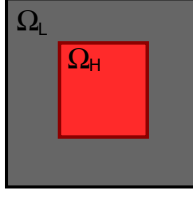


Figure 1: $\Omega = \overline{\Omega}_H \cup \Omega_L$ where Ω_H and Ω_L are highly- and lowly-viscous regions, respectively.

where u , p , and f stand for the velocity, pressure, and body force, respectively. Here, we aim to treat piecewise constant high-contrast viscosity values with the configuration depicted in Figure 1:

$$v(x) = \begin{cases} m \gg 1, & x \in \Omega_H, \\ 1, & x \in \Omega_L. \end{cases} \quad (2)$$

Piecewise constant high-contrast viscosity values are utilized in applications in geodynamics [1, 2, 3] and polymer melting in plastics industry through the process of single screw extrusion [4, 5]. High-contrasts are realistic in these applications. For instance, contrasts up to 10^9 and 10^{12} are used in single screw extrusion applications; see [4, p. 51] and [5, p. 185 and Fig. 3].

The discontinuity and the high-contrast values in the viscosity values cause loss of robustness of preconditioners. Aksoylu and Beyer have shown in [6, 7] that the roughness of coefficients creates serious complications for the diffusion equation with such coefficients in the operator theory framework. Moreover, it was shown in [6] that the standard elliptic regularity in the smooth coefficient case fails to hold. Moreover, the domain of the diffusion operator heavily depends on the regularity of the coefficients. Similar complications also arise in the Stokes case. In this article, we address these complications and show rigorous justification of the methods given in [8] through the help of robust preconditioning. For that, we construct a robust preconditioner based on the one proposed in [9], which we call as the Aksoylu-Graham-Klie-Scheichl (AGKS) preconditioner, which originates from the family of robust preconditioners constructed for the high-contrast diffusion equation under finite element discretization by Aksoylu et al. in [10]. It was proven and numerically verified to be m - and h -robust simultaneously for the different discretizations of the same problem and also for different problems; see [11], [12],[8]. One of the strengths of our proposed preconditioner is *rigorous justification* obtained through the usage of singular perturbation analysis (SPA). Such dramatic extensions rely on the generality of the employed SPA. In this article, we aim to bring the same rigorous preconditioning technology to *vector valued* problems such as the Stokes equation. We extend the usage of AGKS preconditioner to the solution of (1).

The componentwise treatment of the discretization of (1) gives rise to the following systems of equations:

$$\begin{bmatrix} K^x(m) & 0 & (B^x)^t \\ 0 & K^y(m) & (B^y)^t \\ B^x & B^y & 0 \end{bmatrix} \begin{bmatrix} u^x \\ u^y \\ p \end{bmatrix} = \begin{bmatrix} f^x \\ f^y \\ 0 \end{bmatrix}, \quad (3)$$

where $K^* = K^x = K^y$ are the scalar diffusion matrices, and B^x and B^y represent the weak derivatives in x and y directions, respectively. We apply the AGKS preconditioning idea to the K^x and K^y blocks by further decomposing each of them as the following 2×2 block system; see [12, Eqn.

11], [11, Eqn. 4], [9, Eqn. 3]:

$$K^*(m) = \begin{bmatrix} K_{HH}^*(m) & K_{HL}^* \\ K_{LH}^* & K_{LL}^* \end{bmatrix}, \quad (4)$$

where the degrees of freedom (DOF) are identified as *high* and *low* based on the viscosity value in (2) and K_{HH}^* , K_{HL}^* , K_{LH}^* , and K_{LL}^* denote couplings between the high-high, high-low, low-high, and low-low DOF, respectively. The exact inverse of K^* can be written as:

$$K^{*-1} = \begin{bmatrix} I_{HH} & -K_{HH}^{*-1}K_{HL}^* \\ 0 & I_{LL} \end{bmatrix} \begin{bmatrix} K_{HH}^{*-1} & 0 \\ 0 & S^{*-1} \end{bmatrix} \begin{bmatrix} I_{HH} & 0 \\ -K_{LH}^*K_{HH}^{*-1} & I_{LL} \end{bmatrix}, \quad (5)$$

where I_{HH} and I_{LL} denote the identity matrices of the appropriate dimension and the Schur complement S^* is explicitly given by:

$$S^*(m) = K_{LL}^* - K_{LH}^*K_{HH}^{*-1}(m)K_{HL}^*. \quad (6)$$

The AGKS preconditioner is defined as follows:

$$\hat{K}^{*-1}(m) := \begin{bmatrix} I_{HH} & -K_{HH}^{\infty\dagger}K_{HL}^* \\ 0 & I_{LL} \end{bmatrix} \begin{bmatrix} K_{HH}(m)^{*-1} & 0 \\ 0 & S^{\infty-1} \end{bmatrix} \begin{bmatrix} I_{HH} & 0 \\ -K_{LH}^*K_{HH}^{\infty\dagger} & I_{LL} \end{bmatrix}, \quad (7)$$

where $K_{HH}^{\infty\dagger}$ and S^∞ are the asymptotic values of K_{HH}^{*-1} and S^* , respectively; see [9, Lemma 1].

1.1. Design idea of the preconditioner

In the saddle point system (3), $(1, 1)$ -block $K(m)$ is the only block that contains the contrast size m . The contrast is due to the presence of both low ($\mathcal{O}(1)$) and high ($\mathcal{O}(m)$) magnitude partial differential equation (PDE) coefficients. This disproportionate coupling leads to small ($\mathcal{O}(m^{-1})$) eigenvalues in the diagonally scaled stiffness matrix. In a high-contrast elliptic PDE, the solver issues, in particular the loss of robustness, are largely due to those small eigenvalues. The treatment of the coupling between DOF associated to low and high PDE coefficients is a delicate task. It would be ideal to decouple the problem without complications. Hence, the *design idea* of the AGKS preconditioner is based on *decoupling*. This enables us to create blocks in the system matrix associated to low and high magnitude DOF that are entirely of $\mathcal{O}(1)$ and $\mathcal{O}(m)$, respectively. The AGKS preconditioner's *decoupling* role becomes more and more conspicuous as $m \rightarrow \infty$ and that is why the effectiveness of the preconditioner increases for m in the asymptotic regime. Once the decoupling is in place, the AGKS preconditioner employs multigrid (MG) because it can effectively handle both blocks.

When the contrast size in $K(m)$ is treated properly as above, the need for a sophisticated preconditioner for S can be eliminated. More precisely, S can simply be handled by a scaled pressure mass matrix (PMM). This is one of the main distinguishing features of AGKS among other available Stokes preconditioners. Consequently, we are able to construct an effective preconditioner for the high-contrast Stokes equation for which we numerically accomplish the contrast size and mesh size robustness simultaneously. Its effectiveness is supported by rigorous justification which involves SPA. The flexibility of the utilized SPA allowed us to transfer our established results for the high-contrast diffusion equation to the Stokes case.

The remainder of the paper is structured as follows. In Section 2, we describe p-Uzawa, p-SCR, and p-Minres solvers and present a convergence result for the p-Uzawa solver. In Section 3, we comparatively study the performance of the AGKS preconditioner against MG, used under the above solvers. We highlight important aspects of robust preconditioning and draw some conclusions in Section 4.

2. Solver methods

There are many solution methods proposed for the system of equations in (3). Based on where the emphasis is put in the design of a solution method, solving a saddle-point matrix system can be classified into two approaches: *preconditioning and solver*. The *preconditioning approach* aims to construct novel preconditioners for standard solver methods such as Uzawa, Minres, and the Schur complement reduction (SCR) whereas the *solver method approach* aims to construct a solver by sticking with standard preconditioners such as MG for the K matrix and PMM or least-squares (LSQR) commutator (BFBt) preconditioner for the S matrix. See [8, Section 15.1.1] for the detailed literature review of both approaches.

The Ladyzhenskaya-Babuska-Brezzi (LBB) stability of Stokes discretizations plays an important role in the utilization of weak formulations to solve (1). Thus, we start by stating the LBB stability of our discretization, which is given in [13] for high-contrast viscosity:

$$\sup_{u_h \in V_h} \frac{(\operatorname{div} u_h, p_h)}{\|u_h\|_V} \geq c_{LBB} \|p_h\|_Q, \quad p_h \in Q_h.^2 \quad (8)$$

There are many solution methods for the indefinite saddle point problem (3). We concentrate on three different solver methods: the p-Uzawa, p-SCR, and p-Minres. We test the performance the AGKS preconditioner with these solver methods. First, we establish two spectral equivalences: between the velocity stiffness matrix K and the AGKS preconditioner and between the Schur complement matrix S and the scaled PMM. Note that the constant c_{LBB} in (8) is directly used for the spectral equivalence of S in the following.

Lemma 2.1. *Let \hat{K} and \hat{S} denote the AGKS preconditioner and the scaled PMM. Then, for sufficiently large m , the following spectral equivalences hold:*

$$(a) \quad (1 - cm^{-1/2})(\hat{K}u, u) \leq (Ku, u) \leq (1 + cm^{-1/2})(\hat{K}u, u), \quad (9)$$

$$(b) \quad c_{LBB}^2(\hat{S}p, p)_Q \leq (Sp, p) \leq d(\hat{S}p, p)_Q, \quad (10)$$

where the constant c is independent of m , and c_{LBB} is the constant in (8) which is independent of m and h .

Proof. The proof of (a) and (b) can be found in [8, Lemma 15.1 (a)] and [13, Thm. 6], respectively. \square

For the p-Uzawa and p-Minres solvers, we present convergence and conditioning results based on the above spectral equivalences.

²The associated spaces and weighted norms are defined as follows:
 $V := [H_0^1(\Omega)]^d$, $Q := \{p \in L^2(\Omega) : (v^{-1}p, 1) = 0\}$, $\|u\|_V := (v\nabla u, \nabla v)^{\frac{1}{2}}$, $u \in V$, $\|p\|_Q := (v^{-1}p, p)^{\frac{1}{2}}$, $p \in Q$.

2.1. The preconditioned Uzawa solver

The Uzawa algorithm is a classical solution method which involves block factorization with forward and backward substitutions. Here, we use the preconditioned inexact Uzawa method described by [14]. The system (3) can be block factorized as follows:

$$\begin{bmatrix} K(m) & 0 \\ B & -I \end{bmatrix} \begin{bmatrix} I & K(m)^{-1}B^t \\ 0 & S(m) \end{bmatrix} \begin{bmatrix} u \\ p \end{bmatrix} = \begin{bmatrix} f \\ 0 \end{bmatrix}. \quad (11)$$

Let (u^k, p^k) be a given approximation of the solution (u, p) . Using the block factorization (11) combined with a preconditioned Richardson iteration, one obtains:

$$\begin{bmatrix} u^{k+1} \\ p^{k+1} \end{bmatrix} = \begin{bmatrix} u^k \\ p^k \end{bmatrix} + \begin{bmatrix} I & -K^{-1}B^tS^{-1} \\ 0 & S^{-1} \end{bmatrix} \begin{bmatrix} K^{-1} & 0 \\ BK^{-1} & -I \end{bmatrix} \left(\begin{bmatrix} f \\ 0 \end{bmatrix} - \mathcal{A} \begin{bmatrix} u^k \\ p^k \end{bmatrix} \right). \quad (12)$$

This leads to the following iterative method:

$$u^{k+1} = u^k + w^k - \hat{K}^{-1}B^t z^k, \quad (13a)$$

$$p^{k+1} = p^k + z^k, \quad (13b)$$

where $w^k := \hat{K}^{-1}r_1^k$, $r_1^k := f - Ku^k - B^t p^k$, and $z^k := \hat{S}B(w^k + u^k)$. Computing z^k involves ℓ iterations of pCG. In this computation, since the assembly of S is prohibitively expensive, first we replace it by \tilde{S} . Then, we utilize the preconditioner \hat{K} for K and \hat{S} for \tilde{S} where the explicit formula is given by:

$$\tilde{S} := B\hat{K}^{-1}B^t. \quad (14)$$

Thus, the total number of applications of \hat{K}^{-1} in (13a) and (13b) becomes $\ell + 2$. We refer the outer-solve (one Uzawa iteration) as steps (13a) and (13b) combined. In particular, we call the computation of z^k as an S -solve; see Table 1. The stopping criterion of the S -solve plays an important role for the efficiency of the Uzawa method and it is affected by the accuracy of \hat{K} ; see the analysis in [14, Sec. 4]. In Section 2.2, we present the convergence analysis of p-Uzawa method when we use the AGKS preconditioner for a velocity stiffness matrix. Following the results obtained from this analysis, we determine the stopping criterion of the S -solve as follows:

Let r_p^i be the residual of the S -solve at iteration i . Then, we abort the iteration when $\frac{\|r_p^i\|}{\|r_p^0\|} \leq \delta_{tol}$ where either $\delta_{tol} = 0.5$ or the maximum iteration reaches 4. For the details about the choice of δ_{tol} , see Section 2.2.1.

2.2. Analysis of the preconditioned Uzawa solver

There have been many convergence analyses of the Uzawa solver in the literature. These studies mostly covered the continuous viscosity case. To the authors' knowledge, the convergence analysis for the discontinuous viscosity case has never been addressed before. The extension of the convergence analysis to the high-contrast viscosity is our novel contribution. The analysis in [14] lays the foundation of our convergence results. Unlike their case of interest, *i.e.*, a continuous (constant) viscosity $\nu \rightarrow 0$, we treat discontinuous (piecewise constant) $\nu|_{\Omega_H} \rightarrow \infty$. It was shown in [14] that the convergence of the p-Uzawa solver with MG preconditioner was independent of ν . This favorable property is due to the ν independent spectral equivalence between the velocity

stiffness matrix and the MG preconditioner. For the case of discontinuous \mathbf{v} , we prove that the p-Uzawa solver with AGKS preconditioner depends on \mathbf{v} ; see (9). Interestingly this dependence turns out to be an advantage for the high-contrast case³ because it lays the foundation of the results in (a) and (b) below. By using (9), we establish three important results:

- (a) *We prove the convergence of the inexact p-Uzawa solver for large viscosity values $\mathbf{v}|_{\Omega_H} = m$.*
- (b) *We prove that the inexact p-Uzawa method converges to the exact one as $m \rightarrow \infty$.*
- (c) *We quantify the convergence rate of the inexact p-Uzawa solver by the viscosity contrast m in (18) and (19) when the AGKS preconditioner is used for the approximation of velocity stiffness matrix.*

We find that the p-Uzawa method is the most suitable solver for reflecting the effectiveness of a preconditioner designed for high-contrast problems. Since viscosity contrast m can be directly incorporated to the convergence rate, a preconditioner that can use large m values to its advantage will be discerned most obviously under the p-Uzawa solver. In fact, we observe the superior performance of the AGKS preconditioner when it is used under the p-Uzawa method.

Our convergence analysis is based on the one given by [14]. We start by defining the following norms:

$$\begin{aligned} \|u\|_{\hat{K}} &:= (\hat{K}u, u)^{\frac{1}{2}} && \text{for } u \in \mathbb{R}^d \\ \|p\|_{\tilde{S}} &:= (\tilde{S}p, p)^{\frac{1}{2}} && \text{for } p \in e^{\perp \mathcal{Q}} \end{aligned}$$

Let $\begin{bmatrix} u \\ p \end{bmatrix}$ be the exact solution of (1) and e^k be the error in the k -th step of the p-Uzawa method:

$$e^k = \begin{bmatrix} e_u^k \\ e_p^k \end{bmatrix} := \begin{bmatrix} u \\ p \end{bmatrix} - \begin{bmatrix} u^k \\ p^k \end{bmatrix}.$$

Define $\delta_{tol} < 1$ to be the prescribed tolerance of the S -solve enforcing:

$$\frac{\|p - p^k\|_{\tilde{S}}}{\|p\|_{\tilde{S}}} \leq \delta_{tol}. \quad (15)$$

Utilizing the spectral equivalence (9), we have the following error estimates for sufficiently large m :

Lemma 2.2. *Consider the inexact p-Uzawa method defined in (12), then we have the following bounds for the error $e^k = (e_u^k, e_p^k)^t$:*

$$\|e_u^{k+1}\|_{\hat{K}} \leq cm^{-1/2}(2 + \delta_{tol})\|e_u^k\|_{\hat{K}} + \delta_{tol}\|e_p^k\|_{\tilde{S}} \quad (16)$$

$$\|e_p^{k+1}\|_{\tilde{S}} \leq cm^{-1/2}(1 + \delta_{tol})\|e_u^k\|_{\hat{K}} + \delta_{tol}\|e_p^k\|_{\tilde{S}}. \quad (17)$$

Proof. The proof can be found in [14, Thm 4.2]. □

³The design of the AGKS preconditioner is centered on asymptotically large values of $\mathbf{v}|_{\Omega_H} = m$. When m is sufficiently large, the AGKS preconditioner becomes m -robust due to the spectral equivalence in (9).

Theorem 2.1. *Let the spectral equivalences in (9) and (10) hold. Then, the error bound for the p-Uzawa solver is given by the following:*

$$\frac{\max\{\|e_u^{k+1}\|_{\hat{K}}, \|e_p^{k+1}\|_{\bar{S}}\}}{\max\{\|e_u^k\|_{\hat{K}}, \|e_p^k\|_{\bar{S}}\}} = \delta_{tol} + \mathcal{O}(m^{-1/2}) \quad (18)$$

$$\frac{\|e_u^k\|_{\hat{K}} + \|e_p^k\|_{\bar{S}}}{\|e_u^0\|_{\hat{K}} + \|e_p^0\|_{\bar{S}}} = \frac{5}{2}\delta_{tol}^k + \mathcal{O}(m^{-1/2}) \quad (19)$$

Proof. One can write (16) and (17) as follows:

$$\begin{bmatrix} \|e_u^{k+1}\|_{\hat{K}} \\ \|e_p^{k+1}\|_{\bar{S}} \end{bmatrix} \leq C \begin{bmatrix} \|e_u^k\|_{\hat{K}} \\ \|e_p^k\|_{\bar{S}} \end{bmatrix} = \begin{bmatrix} cm^{-1/2}(2 + \delta_{tol}) & \delta_{tol} \\ cm^{-1/2}(1 + \delta_{tol}) & \delta_{tol} \end{bmatrix} \begin{bmatrix} \|e_u^k\|_{\hat{K}} \\ \|e_p^k\|_{\bar{S}} \end{bmatrix}.$$

The result in (18) follows from

$$\|C\|_{\infty} = cm^{-1/2}(2 + \delta_{tol}) + \delta_{tol} = \delta_{tol} + \mathcal{O}(m^{-1/2}).$$

In order to prove (19), we need to find an upper bound for $\|C^k\|_1$. For that, we use the spectral decomposition $C = VDV^{-1}$. The proof is completed by using $\|C^k\|_1 \leq \rho(C)^k \|V\|_1 \|V^{-1}\|_1$ and the following estimates:

$$\rho(C) = \delta_{tol} + \mathcal{O}(m^{-1/2}), \quad \|V\|_1 \leq \frac{5}{2} + \mathcal{O}(m^{-1/2}), \quad \|V^{-1}\|_1 = 1.$$

□

Remark 2.1. *For m sufficiently large, it follows from Theorem 2.1 that the p-Uzawa solver always converges when the preconditioner of choice is AGKS. In addition, the contraction factor for the inexact Uzawa method converges to that of the exact one; $\delta_{tol} + \mathcal{O}(m^{-1/2})$ and δ_{tol} , respectively. We can deduce that only one iteration of pCG with the AGKS preconditioner is enough for the accuracy of S-solve in the asymptotic regime⁴. We give the justification of this deduction in Section 2.2.1.*

2.2.1. The choice of optimal δ_{tol}

Let k and ℓ be the number of outer- and S-solve iterations of the p-Uzawa solver. Here we comment on the effect of the choice of δ_{tol} on the total number of iterations for varying m values. An optimal δ_{tol} is chosen so that the total number of p-Uzawa iterations is minimized. In other words, δ_{tol} guarantees not only the convergence, but also the efficiency of the p-Uzawa solver. Let $\varepsilon < 1$ be the tolerance of the p-Uzawa solver and $\beta < 1$ be contraction factor of the S-solve. Using (19) and (15), we have:

$$\rho(C)^k \leq \varepsilon, \quad \beta^{\ell} \leq \delta_{tol}.$$

⁴For the definition of asymptotic regime, see Section 3. Note that the asymptotic regime of the p-Uzawa solver is observed to be $m \geq 10^3$; see Table 1.

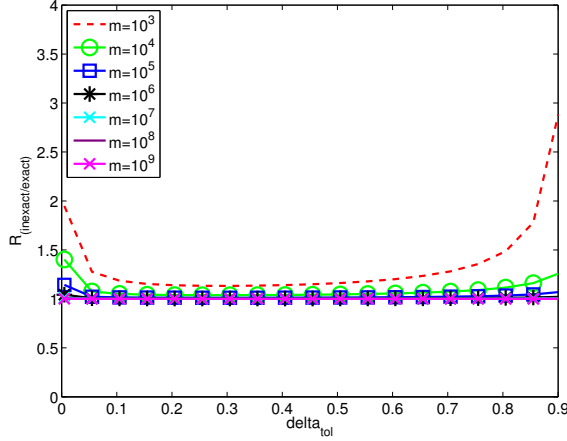


Figure 2: The plot of $R_{inexact/exact}$ for fixed $\beta = 0.8$, and $m \geq 10^3$.

In order to find the optimal δ_{tol} , we minimize the total number of p-Uzawa iterations given by $k\ell$:

$$k\ell \leq \frac{\ln(\epsilon)}{\ln(\rho(C))} \frac{\ln(\delta_{tol})}{\ln(\beta)} = \frac{\ln(\epsilon)}{\ln(\beta)} \frac{\ln(\delta_{tol})}{\ln(\rho(C))} =: iter_{exact} R_{inexact/exact}.$$

Here $R_{inexact/exact}$ represents the ratio of the number of iterations of the p-Uzawa and exact Uzawa solvers. It suffices to minimize $R_{inexact/exact}$ to figure out the range for optimal δ_{tol} . We present the plot of $R_{inexact/exact}$ for a generic constant $c = 1$ ⁵ in Figure 2. As m value gets larger, specifically for $m \geq 10^3$, we observe that $R_{inexact/exact}$ reaches its minimum value for almost all δ_{tol} . As m gets larger, the fact that the smallest value of $R_{inexact/exact} \rightarrow 1$ indicates that the total number of p-Uzawa iterations goes to that of the exact one. Since it was pointed out by [14] that $\delta_{tol} = 0.5$ is an optimal value for the MG preconditioner, we choose the same δ_{tol} in p-Uzawa in order to make a fair comparison between AGKS and MG.

2.3. The preconditioned Schur complement reduction (p-SCR) solver

The p-SCR is a direct method which decouples the velocity and pressure equations. This method involves the following block Gaussian eliminated system:

$$\begin{bmatrix} K(m) & B^t \\ 0 & S(m) \end{bmatrix} \begin{bmatrix} u \\ p \end{bmatrix} = \begin{bmatrix} f \\ f^p \end{bmatrix}, \quad (20)$$

where $f^p = BK^{-1}f$. Applying backward substitution, one obtains the following decoupled system of equations:

$$\text{Solve for } p: \quad Sp = f^p, \quad (21)$$

$$\text{Solve for } u: \quad Ku = f - B^t p. \quad (22)$$

⁵The constant c is from the explicit expression of $\mathcal{O}(m^{-1/2})$ in (9). A numerical study reveals that $R_{inexact/exact}|_{c=1}$ is an upper bound for $R_{inexact/exact}$.

The systems in (21) and (22) are solved by preconditioned Krylov solvers. Since the explicit construction of S is required in each step of these subspace methods, we replace the system in (21) by the following equation:

$$\tilde{S}p = f^p, \quad (23)$$

where \tilde{S} is the approximation of S by $B\hat{K}^{-1}B^t$ as in (14), and \hat{K} is the preconditioner for K . The methods applied to solve (21) and (22) are referred as the S -solve and the K -solve, respectively; see Table 2. Since the p-SCR solver is a direct method, the convergence of the S -solve highly depends on the accuracy of the K^{-1} approximation used in each step. Therefore, instead of one application of \hat{K}^{-1} (as in the case of p-Uzawa solver), we use an accurate approximation of K^{-1} in each step of the S -solve. This is the main distinction between the usage of p-SCR and p-Uzawa solvers.

2.4. The preconditioned Minres solver

The p-Minres is a popular iterative method applied to the system (3). Let $v := \begin{bmatrix} u \\ p \end{bmatrix}$. With the given initial guess $v^0 := \begin{bmatrix} u^0 \\ p^0 \end{bmatrix}$ where $p^0 \in e^{\perp \varrho}$ and with the corresponding error $r^0 := v - v^0$, the p-Minres solver computes:

$$v^k = \underset{v \in v^0 + \mathcal{H}^k(\mathcal{B}^{-1}\mathcal{A}, \tilde{r}^0)}{\operatorname{argmin}} \left\| \mathcal{B}^{-1} \left(\begin{bmatrix} f \\ 0 \end{bmatrix} - \mathcal{A}v \right) \right\|.$$

Here, $\tilde{r}^0 = \mathcal{B}^{-1}r^0$ and $\mathcal{H}^k = \operatorname{span}\{\tilde{r}^0, \mathcal{B}^{-1}\mathcal{A}\tilde{r}^0, \dots, (\mathcal{B}^{-1}\mathcal{A})^k\tilde{r}^0\}$, and the preconditioner has the following block diagonal structure:

$$\mathcal{B} = \begin{bmatrix} \hat{K} & 0 \\ 0 & \hat{S} \end{bmatrix}, \quad (24)$$

where \hat{K} and \hat{S} are the preconditioners for K and S , respectively. In each step of the p-Minres solver the above preconditioner is applied in the following fashion: for the K -block one application of \hat{K} and for the S -block several applications of pCG to the \tilde{S} -system⁶ with \hat{S} as the preconditioner. The p-Minres iterations are called outer-solve whereas the pCG solve for the \tilde{S} -system is called inner-solve.

The convergence rate of the p-Minres method depends on the condition number of the preconditioned matrix, $\mathcal{B}^{-1}\mathcal{A}$. Combining the spectral equivalences given in (9) and (10) with the well-known condition number estimate, we obtain:

$$\kappa_{\mathcal{B}}(\mathcal{B}^{-1}\mathcal{A}) \leq \frac{\max\{(1 + cm^{-1/2}), d\}}{\min\{(1 - cm^{-1/2}), c_{LBB}^2\}}$$

It immediately follows that the convergence rate of the p-Minres method is independent of m asymptotically.

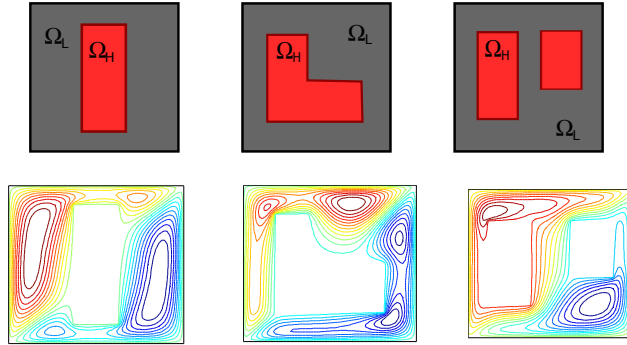


Figure 3: The streamline plot of the high-contrast Stokes equation for three different high-viscosity island configurations; (left) rectangular, (middle) L-shaped, and (right) two disconnected islands.

3. Numerical experiments

The goal of the numerical experiments is to compare the performance of the AGKS and MG preconditioners by using three different solvers: p-Uzawa, p-SCR and p-Minres. We employ a V(1,1)-cycle, with point Gauss-Seidel (GS) smoother. A direct solver is used for the coarsest level.

We consider cavity flow depicted in Figure 3 with enclosed boundary conditions with right hand side functions $f = 1$ and $g = 0$ on a 2D domain $[-1, 1] \times [-1, 1]$; also see [8, Section 15.3]. The high-contrast viscosity values we test originate from the *Sinker* model introduced by May and Moresi [1]. Physically, it corresponds to a slab subduction (or sinking block) application. The *Sinker* model has been adopted by the geodynamics community as a benchmark problem; see [1, Fig. 2], [2, Sec. 4.3], and [3, Sec. 5.2] for 3D applications. The *Sinker* model with second order Stokes formulation is used in [2] and [15]. In addition, contrasts up to 10^9 and 10^{12} are realistic values utilized in single screw extrusion applications; see [4, p. 51] and [5, p. 185 and Fig. 3].

The other formulation of the Stokes equation that is different from (1) is the so-called “velocity-stress-pressure” [16, Equ. (7.15)] or the “stress-divergence” formulation [17, p. 277]. This is a first order formulation of Stokes equation and has been used in [1], [3], and [18], whereas (1) is a second order formulation. The two formulations are equivalent; see [17, p. 277]. But, systems arising after discretization are different. This fact is also mentioned in [17, p. 277]. Our preconditioner is designed for a second order formulation which is widely used in the numerical analysis community. To extend the preconditioner to a first order formulation is beyond the scope of this paper.

For each level of refinement, we present the number of iteration corresponding to each solve (outer-solve and S -solve; S -solve and K -solve, outer-solve and inner-solve for p-Uzawa, p-SCR, and p-Minres iterations, respectively). For the p-Uzawa and p-Minres methods, we only report the performance of AGKS preconditioner; see [8] for the MG performance, and the further comparisons. In the tables, N , N_S , and N_{K^*} stand for the number of DOF in \mathcal{A} , S , and K^* systems,

⁶ Here, $\tilde{S} = B\hat{K}^{-1}B^t$ stands for the approximation of S . Since S is replaced by \tilde{S} , this turns the p-Minres algorithm to an inexact one; see the inexactness discussion in [8, Section 15.3.2].

Table 1: Number of iterations for p-Uzawa with AGKS preconditioning, Q_2-Q_1 , rectangular mesh.

$N \setminus m$	10^0	10^1	10^2	10^3	10^4	10^5	10^6	10^7	10^8	10^9	$N_S \setminus m$	10^0	10^1	10^2	10^3	10^4	10^5	10^6	10^7	10^8	10^9	
outer-solve											S-solve											
659	24	15	14	14	14	14	14	14	14	14	81	3	2	3	3	3	3	3	3	3	3	3
2467	38	21	18	19	18	18	18	18	18	18	289	3	3	3	3	3	3	3	3	3	3	3
9539	47	31	16	16	15	15	15	15	15	15	1089	1	1	3	1	1	1	1	1	1	1	1
37507	70	50	17	16	15	15	15	15	15	15	4225	1	1	3	1	1	1	1	1	1	1	1

Table 2: Number of iterations for p-SCR, Q_2-Q_1 , rectangular mesh. (top) MG, (bottom) AGKS.

$N_S \setminus m$	10^0	10^1	10^2	10^3	10^4	10^5	10^6	10^7	10^8	10^9	$N_{K^*} \setminus m$	10^0	10^1	10^2	10^3	10^4	10^5	10^6	10^7	10^8	10^9	
S-solve											K-solve											
81	10	14	14	14	14	14	14	14	14	14	289	7	7	7	7	7	7	7	7	7	7	7
289	10	15	15	15	15	15	15	15	15	15	1089	6	7	7	7	7	7	7	7	7	7	7
1089	11	16	17	17	17	17	17	17	17	17	4225	6	7	7	7	7	7	7	7	7	7	7
4225	12	17	18	18	18	18	18	18	18	18	16641	6	7	7	7	7	7	7	7	7	7	7
81	10	14	14	14	14	14	14	14	14	14	289	12	8	5	3	3	3	1	1	1	1	1
289	10	15	15	15	15	15	15	15	15	15	1089	17	10	6	4	3	3	2	1	1	1	1
1089	11	16	17	17	17	17	17	17	17	17	4225	24	14	7	5	3	3	1	1	1	1	1
4225	12	17	18	18	18	18	18	18	18	18	16641	32	17	8	5	3	3	2	1	1	1	1

respectively. We enforce an iteration bound of 200. If the method seems to converge slightly beyond this bound, we denote it by $*$.

In analyzing m -robustness, we observe a special feature. The iteration count remains fixed when m becomes larger than a certain threshold value. We define the notion of *asymptotic regime* to indicate m values bigger than this threshold. Identifying an asymptotic regime is desirable because it immediately indicates m -robustness.

Table 3: Number of iterations for p-SCR, Q_2-Q_1 , skewed mesh ($\frac{\pi}{4}$). (top) MG, (bottom) AGKS.

$N_S \setminus m$	10^0	10^1	10^2	10^3	10^4	10^5	10^6	10^7	10^8	10^9	$N_{K^*} \setminus m$	10^0	10^1	10^2	10^3	10^4	10^5	10^6	10^7	10^8	10^9	
S-solve											K-solve											
81	17	23	27	31	32	32	32	32	32	32	289	8	9	9	9	9	9	9	9	9	9	9
289	20	28	33	38	39	38	38	38	38	38	1089	8	9	10	11	12	12	12	12	12	12	12
1089	22	34	38	43	45	45	44	44	44	44	4225	8	9	11	13	13	13	13	13	13	13	13
4225	25	41	43	47	49	49	49	49	49	49	16641	8	9	12	15	15	15	15	15	15	15	15
81	16	22	25	30	30	31	31	31	31	31	289	16	13	12	12	12	12	14	15	15	16	16
289	18	26	31	38	38	38	37	37	37	37	1089	22	15	14	13	13	14	14	16	16	18	18
1089	20	32	36	41	44	44	43	43	43	43	4225	22	15	14	13	13	14	14	16	16	18	18
4225	22	40	41	45	48	48	48	48	48	48	16641	22	15	14	13	13	14	14	16	16	18	18

We observe that the p-Uzawa method is m -robust as long as the optimal stopping criterion is

Table 4: Number of iterations for p-Minres with AGKS preconditioning, $Q2-Q1$, rectangular mesh.

$N \setminus m$	10^0	10^1	10^2	10^3	10^4	10^5	10^6	10^7	10^8	10^9	$N_{K^*} \setminus m$	10^0	10^1	10^2	10^3	10^4	10^5	10^6	10^7	10^8	10^9
	outer-solve											inner-solve									
659	29	23	18	16	18	16	16	18	20	20	81	20	20	5	5	5	5	5	5	5	5
2467	40	30	17	17	16	16	16	19	19	19	289	20	20	5	5	5	5	5	5	5	5
9539	50	45	20	20	19	16	16	20	20	20	1089	20	20	5	5	5	5	5	5	5	5
37507	70	52	22	20	19	16	16	20	20	20	4225	20	20	5	5	5	5	5	5	5	5

used for the S -solve; see Table 1. This stopping criterion is chosen according to the convergence analysis in Section 2.2. The AGKS preconditioner maintains m - and h -robustness simultaneously when used as a preconditioner for p-Uzawa method. Asymptotically, only one iteration of pCG is sufficient to obtain an accurate S -solve; see Table 1. When we calculate the total number of AGKS applications explained in Section 2.2, we find $15 \times (1 + 2) = 45$. Since this application count remains fixed as the mesh is refined, we infer the h -robustness of the AGKS preconditioner; see Figure 4. When the MG preconditioner is used, on the other hand, the p-Uzawa solver loses m - and h -robustness, which results in unreasonable number of applications of the MG preconditioner in total; see [8, Section 15.3.1].

For the p-SCR method, we apply the pCG method with either AGKS or MG preconditioner for the K -solve, and pCG method with scaled PMM preconditioner for the S -solve (with an accuracy of 5×10^{-6} each.) Since an accurate K -system solution is required for both the K -solve and S -solve, the p-SCR method plays a critical role in revealing the effectiveness of the AGKS and MG as standalone preconditioners. Typically a sophisticated preconditioner such as BFBt is suggested to handle the S system due to complications arising from high-contrast viscosity. We overcome these complications by focusing on an accurate K -solve in each iteration of the S -solve. Therefore, even a simple preconditioner such as scaled PMM maintains m -robustness resulting in a good performance of pCG for the S -solve. But h -robustness was lost; see Table 2. As long as the K -solve is accurate, the preconditioner choice (whether AGKS or MG) does not affect the performance of pCG in S -solve. However, this performance heavily depends on the mesh aspect ratio and the choice of discretization. We obtain the fastest convergence when $Q2-Q1$ discretization is used on a rectangular mesh; see Table 2. For the $Q2-Q1$ discretization, aspect ratio deterioration spoils the h -robustness of the MG preconditioner whereas it spoils the m -robustness of the AGKS preconditioner; see Table 3.

For the p-Minres method, we have taken a novel approach for the S system, and use the inexact p-Minres solver as explained in [8]. We observe that the choice of \hat{K}^{-1} —an application of either MG or AGKS—in the inner-solve dramatically affects the performance inner-solve. Specifically, the scaled PMM preconditioner is m -robust, but not h -robust for the inner-solve with MG, whereas it is both m - and h -robust for inner-solve with AGKS.

When we compare the performance of the AGKS preconditioner under three different solvers, we observe the following results.

The p-Uzawa solver turns out to be the best choice since AGKS preserves both m - and h -robustness regardless of the discretization type, deterioration in the aspect ratio of the mesh, or

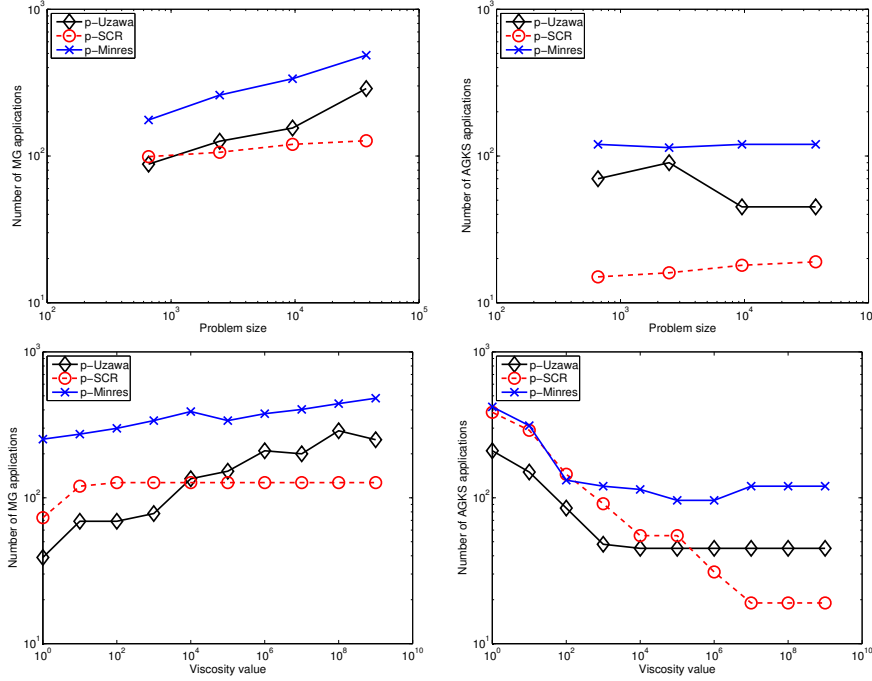


Figure 4: The plot of the number of (top-left) MG applications versus problem size for fixed viscosity value $m = 10^8$, (bottom-left) MG applications versus viscosity value for fixed level = 4 (top-right) AGKS applications vs problem size for fixed viscosity value $m = 10^8$, (bottom-right) AGKS applications versus viscosity value for fixed level = 4.

the island configuration. The change in one of the above only causes increase in the number of iterations, but qualitatively m - and h -robustness are maintained. Moreover, we observe that the asymptotic regime of the p-Uzawa solver starts with the m value 10^3 ; see left-bottom in Figure 4.

The p-SCR solver, on the other hand, becomes the fastest for the problem in consideration with Q_2 - Q_1 discretization in a rectangular mesh. However, the AGKS under the p-SCR solver is not h -robust; see the left column of Table 2. As island configuration changes, the number of iterations of both K - and S -solve increases. In addition to that, as the discretization changes, the m -robustness of PMM for S -solve is lost. Therefore, as the problem gets larger or island configuration becomes more complicated, the p-SCR solver becomes less desirable than p-Uzawa; see bottom-left and top-left in Figure 4. The asymptotic regime of the p-Uzawa solver is $m \geq 10^7$.

The AGKS preconditioner under the p-Minres solver also maintains both m - and h -robustness as the discretization, the aspect ratio of the mesh, or the island configuration change; see Table 4. However, the number of iterations in the p-Minres solver increases dramatically when the mesh is skewed; see [8, Tables 15.9 and 15.10]. Compared to p-Uzawa, one needs a more accurate inner-solve for a convergent p-Minres. In addition, the asymptotic regime of p-Minres solver is $m \geq 10^7$. Combining these three features, p-Minres becomes less desirable compared to p-Uzawa. We observe that p-Minres method has the poorest performance among p-Uzawa and p-SCR methods in terms of number of AGKS and MG applications. However, this solver is potentially useful for large size problems as the AGKS preconditioner maintains h -robustness.

4. Conclusion

The novelty of the preconditioner lies in its design idea. The preconditioner plays the role of a “decoupler” in order to prevent the complications caused by the high-contrast values. Once this decoupling of $\mathcal{O}(m)$ and $\mathcal{O}(1)$ blocks is in place, standard MG can handle both blocks effectively. If this decoupling is not in place, MG fails and this is what we want to establish in this article. Furthermore, when the high-contrast in the $K(m)$ block is treated properly, the need for a sophisticated preconditioner for the Schur complement can be eliminated. Only after the use of the AGKS preconditioner, the standard solver technology for smooth PDE coefficients can be exploited for the high-contrast case.

Consequently, we are able to construct an effective preconditioner for the high-contrast Stokes equation for which we numerically accomplish the contrast size and mesh size robustness simultaneously. Its effectiveness is supported by rigorous justification which involves SPA. The flexibility of the utilized SPA allowed us to transfer our established results for the high-contrast diffusion equation to the Stokes case.

We also investigate the MG and AGKS sensitivity against the coarsest grid solve. We had observed that MG loses m - and h -robustness under $P1$ -discretization when direct solve is replaced by 200 SSOR iterations; see [9, Tables 9 and 10]. When the discretization is changed to be $Q2$, we also observe a similar adverse behavior with 200 SSOR iterations. When the coarsest grid solve is chosen to be CG, MG still is ineffective because of the loss of m - and h -robustness. On the other hand, the performance of AGKS is affected minimally with SSOR coarsest grid solve. More precisely, it still maintains m - and h -robustness, however, asymptotic regime is now $m \geq 10^9$ (instead of $m \geq 10^7$). The performance of AGKS even improves with CG coarsest grid solve. We can infer one more robustness of the AGKS preconditioner. Namely, AGKS is *robust with respect to the choice of coarsest grid solve*. For a fair comparison, we report the case when direct solve is chosen for both preconditioners.

References

- [1] D. A. May, L. Moresi, Preconditioned iterative methods for Stokes flow problems arising in computational geodynamics, *Physics of the Earth and Planetary Interiors* 171 (2008) 33–47.
- [2] M. ur Rehman, T. Geenen, C. Vuik, G. Segal, S. MacLachlan, On iterative methods for the incompressible Stokes problem, *International Journal for Numerical Methods in Fluids* (2010) 1731–1751.
- [3] M. Furuichi, D. A. May, P. J. Tackley, Development of a Stokes flow solver robust to large viscosity jumps using a schur complement approach with mixed precision arithmetic, *J. Comput. Phys.* 230 (2011) 8835–8851.
- [4] A. Altinkaynak, Three-Dimensional Finite Element Simulation of Polymer Melting and Flow in a Single-Screw Extruder: Optimization of Screw Channel Geometry, Ph.D. thesis, Michigan Technological University, Michigan, USA, 2010.
- [5] A. Altinkaynak, M. Gupta, M. A. Spalding, S. L. Crabtree, Melting in a Single Screw Extruder: Experiments and 3D Finite Element Simulations, *Intern. Polymer Processing* 26 (2011) 182–196.
- [6] B. Aksoylu, H. R. Beyer, Results on the diffusion equation with rough coefficients, *SIAM J. Math. Anal.* 42 (2010) 406–426.
- [7] B. Aksoylu, H. R. Beyer, On the characterization of the asymptotic cases of the diffusion equation with rough coefficients and applications to preconditioning, *Numer. Funct. Anal. Optim.* 30 (2009) 405–420.
- [8] B. Aksoylu, Z. Unlu, Numerical study of the high-contrast Stokes equation and its robust preconditioning, in: G. A. Anastassiou, O. Duman (Eds.), *Advances in Applied Mathematics and Approximation Theory*, volume 41

of *Springer Proceedings in Mathematics & Statistics*, Springer, 2013, pp. 237–262. DOI: 10.1007/978-1-4614-6393-1.

- [9] B. Aksoylu, I. G. Graham, H. Klie, R. Scheichl, Towards a rigorously justified algebraic preconditioner for high-contrast diffusion problems, *Comput. Vis. Sci.* 11 (2008) 319–331.
- [10] B. Aksoylu, H. Klie, A family of physics-based preconditioners for solving elliptic equations on highly heterogeneous media, *Appl. Num. Math.* 59 (2009) 1159–1186.
- [11] B. Aksoylu, Z. Yeter, Robust multigrid preconditioners for cell-centered finite volume discretization of the high-contrast diffusion equation, *Comput. Vis. Sci.* 13 (2010) 229–245.
- [12] B. Aksoylu, Z. Yeter, Robust multigrid preconditioners for the high-contrast biharmonic plate equation, *Numer. Linear Algeb. Appl.* 18 (2011) 733–750.
- [13] M. A. Olshanskii, A. Reusken, Analysis of a Stokes interface problem, *Numer. Math.* 103 (2006) 129–149.
- [14] J. Peters, V. Reichelt, A. Reusken, Fast iterative solvers for discrete Stokes equations, *SIAM J. Sci. Comput.* 27 (2005) 646–666.
- [15] M. ur Rehman, Fast Iterative Methods for the Incompressible Navier-Stokes Equations, Ph.D. thesis, Delft University of Technology, The Netherlands, 2010.
- [16] P. B. Bochev, M. D. Gunzburger, Least-Squares Finite Element Methods, *Applied Mathematical Sciences*, Volume 166, Springer, 2009.
- [17] H. C. Elman, D. J. Silvester, A. J. Wathen, Finite elements and fast iterative solvers: with applications in incompressible fluid dynamics, *Numerical Mathematics and Scientific Computation*, Oxford University Press, 2005.
- [18] T. Geenen, M. ur Rehman, S. P. MacLachlan, G. Segal, C. Vuik, A. P. van den Berg, W. Spakman, Scalable robust solvers for unstructured FE geodynamic modeling applications: Solving the Stokes equation for models with large localized viscosity contrasts, *Geochemistry, Geophysics, Geosystems* 10 (2009) 1–12.